RESEARCH ARTICLE | MARCH 26 2025

Disentangling signal contributions in two-dimensional electronic spectroscopy in the pump–probe geometry

Special Collection: David Jonas Festschrift

Daniel Timmer ; Daniel C. Lünemann ; Antonietta De Sio ; Giulio Cerullo ; Christoph Lienau

J. Chem. Phys. 162, 124202 (2025)
https://doi.org/10.1063/5.0256813

The Journal of Chemical Physics ARTICLE pubs.aip.org/aip/jcp

Disentangling signal contributions in two-dimensional electronic spectroscopy in the pump–probe geometry

Cite as: J. Chem. Phys. 162, 124202 (2025); doi: 10.1063/5.0256813
Submitted: 7 January 2025 • Accepted: 2 March 2025 •
Published Online: 26 March 2025

Daniel Timmer,[1,a)] Daniel C. Lünemann,[1] Antonietta De Sio,[1,2] Giulio Cerullo,[3,4] and Christoph Lienau[1,2,a)]

AFFILIATIONS

[1] Institut für Physik, Carl von Ossietzky Universität Oldenburg, 26129 Oldenburg, Germany
[2] Center for Nanoscale Dynamics (CENAD), Carl von Ossietzky Universität Oldenburg, 26129 Oldenburg, Germany
[3] Istituto di Fotonica e Nanotecnologie-CNR, Piazza L. da Vinci 32, 20133 Milano, Italy
[4] Dipartimento di Fisica, Politecnico di Milano, Piazza L. da Vinci 32, 20133 Milano, Italy

Note: This paper is part of the JCP Special Topic, David Jonas Festschrift.
[a)]**Authors to whom correspondence should be addressed:** daniel.timmer@uol.de and christoph.lienau@uni-oldenburg.de

ABSTRACT

Since its introduction almost three decades ago, two-dimensional electronic spectroscopy (2DES) has evolved into a mature and powerful technique to reveal the inner workings of quantum systems with high temporal and spectral resolution. In general, this technique can isolate different contributions to the nonlinear response and provides access to different dynamical quantum pathways of the system evolution. Such isolation of pathways can be achieved in different experimental geometries. In its original, fully noncollinear implementation, directional phase matching allows for such signal isolation, while in the modern commonly employed pump–probe geometry, experimentally challenging phase-cycling schemes are employed. Here, we show how rephasing, non-rephasing, and zero- and double-quantum 2DES signals can be isolated in the pump–probe geometry without a need for phase-cycling. For this, we utilize established causality restrictions of the nonlinear response, allowing us to separate the different contributions in the spectral domain. We demonstrate this using data recorded for a molecular J-aggregate, acting as an effective three-level system. This approach bridges the gap between the capabilities of shaper-based and fully noncollinear 2DES and experimentally simpler implementations, such as those based on birefringent common-path interferometers.

I. INTRODUCTION

Two-dimensional electronic spectroscopy (2DES)[1–4] is an established third-order nonlinear spectroscopy technique that offers uniquely deep insights into coherent and incoherent couplings and many-body interactions in atomic, molecular, and condensed matter quantum systems. Introduced in 1998 in pioneering work by the Jonas group,[4] it is the optical analog to two-dimensional nuclear magnetic resonance spectroscopy.[5] In its simplest implementation, it can be considered as an extension of pump–probe spectroscopy,[1] which provides resolution not only in the detection but also in the excitation energy. By using a phase-stable pump pulse pair with a controllable time delay τ, the "coherence time," access to the different excitation pathways of the quantum system is provided via a Fourier transform (FT). This results in energy–energy maps that correlate the excitation and detection energy as a function of the "waiting time," the delay between the second pump pulse and the probe. In an oversimplified picture, one may consider 2DES as an excitation-energy resolved pump–probe measurement, in which ubiquitous cross-peaks can directly indicate interactions between spectrally distinct resonances. In 2DES, the high frequency resolution is combined with a high time resolution that is only limited by the employed pulse durations. Importantly, persistent oscillations of these cross-peaks along the waiting time axis distinguish coherent

from incoherent interactions. As such, 2DES is ideally suited to access the quantum coherent evolution in complex and strongly interacting systems and phenomena such as many-body interactions in semiconductors[2,6,7] or coherent and incoherent couplings in hybridized light–matter systems.[8–11]

Different experimental implementations of 2DES exist.[2,3] Their most fundamental differences lie in the geometry under which the two pump pulses and the probe are impinging onto the sample and how the desired nonlinear signal is isolated. In its first realization,[4] the so-called BoxCARS geometry, all three laser pulses are fully noncollinear and are aligned such that they form three of the corners of a box arrangement.[2–4] The nonlinear four-wave mixing signal is then emitted in a background-free direction into the fourth corner due to directional phase-matching constraints. It is then heterodyned with a fourth local oscillator pulse to obtain the complex emitted nonlinear electric field. This implementation offers the greatest versatility, such as independent control of amplitude, polarization, and phase of the laser pulses, although at the price of being experimentally complex. In addition, signals can suffer from certain artifacts, such as directional filtering.[12,13]

One major advantage of the BoxCARS approach is that certain quantum pathways can be isolated. While in third-order pump–probe experiments, excitation of the system by the pump pulse occurs via two simultaneous field interactions, in 2DES, each of the pump pulses only interacts once.[14,15] During τ, the system, therefore, evolves in a coherence between the ground and an excited state, requiring interferometric stability of the excitation pulse pair to resolve this coherence, which oscillates at optical frequencies. An important aspect of 2DES is that the system third-order nonlinear polarization that is induced by the probe laser may either evolve with the same sign (non-rephasing signal) or evolve with the opposite sign (rephasing signals) of its oscillation frequency as the coherence that is initiated by the first pump. Since phase-matching dictates that in the BoxCARS geometry, rephasing (R) and non-rephasing (NR) signals are emitted in different directions, they can be measured individually, usually by a change in the ordering of the first two pulses. This is important since a R pathway represents a photon echo-type signal, in which possible inhomogeneous broadening effects in an ensemble of quantum emitters are suppressed by the reversed system evolution.[16] The separation of R and NR pathways may be desirable since, in addition to separating homogeneous from inhomogeneous broadening, it offers insights into many-body interactions in semiconductors[17,18] or can distinguish between the ground and excited state vibrational wavepacket dynamics in molecules.[19]

While in all these cases, the two pump pulses, i.e., the first two field interactions, have excited the system, resulting in so-called single-quantum (1Q) 2DES signals, a fundamentally different class of signals can be obtained in the BoxCARS geometry.[20] In double-quantum (2Q) 2DES,[2,21] the first two interactions, usually interacting with the sample without any relative delay, prepare the system in a 2Q coherence between the ground and a doubly excited state without creating an intermediate population state. Its evolution is then probed by the third pulse by converting the 2Q coherence into a 1Q coherence that can then be measured. Such signals are able to directly probe the energies and dephasing rates of higher-lying states, e.g., two-exciton states in molecular aggregates,[22,23] higher ranks of a Tavis–Cummings ladder,[24] or doubly excited states in semiconductors[25] and quantum wells.[26] In a similar fashion, zero-quantum (0Q) signals can be measured, probing the coherence within the ground or excited state manifold. Such signals have also been used, e.g., to probe valley coherence in transition metal dichalcogenide monolayers[27] or exciton hybridization in a TMD heterostructure.[28] While these 0Q and 2Q signals represent third-order responses, recent developments show that also higher-order excitations can be accessed when going beyond $\chi^{(3)}$.[24,29–33]

A conceptually simpler implementation of 2DES is the partially collinear pump–probe geometry, employing a collinearly propagating, interferometrically stable pump pulse pair.[1,3] As in a standard pump–probe experiment, the nonlinear signal is then radiated into the phase-matched probe direction. It is, therefore, no longer emitted in a background-free direction but heterodyned by the probe. The nonlinear signal contribution is usually isolated by recording a differential signal that can be obtained via pump pulse chopping. As a consequence of the partially collinear geometry, R and NR signals can no longer be measured separately and are both simultaneously contained in the recorded 2DES maps.[1,14] The resulting signal is of the absorptive type and corresponds to an excitation-energy resolved pump–probe measurement. While automatically phased absorptive 2DES signals are convenient since they allow for a straightforward interpretation of spectral line shapes,[1,14] it may be desirable to maintain the ability to isolate the R and NR contribution as well as to record 0Q and 2Q signals also in this geometry.

Currently, two main experimental approaches exist to generate the collinear pump pulse pair for 2DES: (i) pulse-shaper based[34–36] and (ii) using a birefringent common-path interferometer.[37,38] The pulse-shaper approach, either implemented using acousto-optic programmable dispersive filters[34,36,39] or acousto-optic/liquid crystal modulators in the Fourier plane of a 4f pulse shaper,[35] enables advanced 2DES schemes since it can be used to control the absolute phases ϕ_i of the excitation pulses, e.g., for measurements in the rotating frame, and to implement so-called phase-cycling (PC) schemes. In PC, the absolute phases of one or multiple pulses are varied to specific values such that a linear combination of the recorded data isolates the desired pathway. It has been shown that in partially collinear shaper-based 2DES, R and NR signals can be isolated using PC.[34,40] It has also recently been demonstrated that 2Q and 0Q signals can be recorded for shaper-based 2DES.[41] The second partially collinear 2DES approach utilizes a mechanically tunable common-path interferometer based on birefringent wedges. The Translating Wedge-based Identical pulse eNcoding System (TWINS)[38] exploits the different group delays between ordinary and extraordinary polarizations in a birefringent material to create a delay between two polarization components of an ultrashort laser pulse. This approach has been demonstrated for 2DES using broadband laser spectra in the UV,[42] visible,[38,43] and near-infrared[37] with high time resolution. The TWINS has also found application in recent developments for action-based 2DES,[44,45] usually as the detection interferometer. Recently, we have been able to demonstrate previously lacking PC abilities for the TWINS, enabling to record R, NR, 0Q, and 2Q signals.[22]

Another important implementation, different from those discussed so far, is fully collinear 2DES, offering certain critical

advantages, such as a high spatial resolution.[46–48] Such an implementation, however, requires access to the phase control of all laser pulses and is, therefore, usually experimentally more demanding than an implementation in the pump–probe geometry.

Already earlier, Ogilvie and co-workers introduced a conceptually interesting approach to isolate quantum pathways in partially collinear, shaper-based 2DES.[34] Their approach relied on the imposition of causality on the signals recorded along the detection energy axis. For 2DES signals recorded with impulsive excitation, i.e., with fictitious δ-pulses, causality imposes that the field emitted by the nonlinear polarization that is created by the three pulses can only be emitted after the interaction with the last pulse, usually the probe pulse.[14,15,49] The resulting FT properties of the nonlinear response can then be exploited to isolate R and NR contributions to the 2DES maps obtained using four-step PC of the excitation pulse pair.[34] Such causality imposing was also utilized by Zanni and co-workers to isolate R and NR signals for shaper-based 2D-IR spectroscopy.[50] In both cases, relative phases $\Delta\phi_{21} = \phi_2 - \phi_1 = \left[0, \frac{\pi}{2}, \pi, \frac{3\pi}{2}\right]$ between the two pump pulses have been used and R and NR contributions were obtained from a linear combination of the measurements. These and other examples may give the impression that PC is a requirement for partially collinear 2DES in order to fully unlock access to distinct responses, i.e., to isolate R and NR contributions and to measure 0Q and 2Q signals. Indeed, to the best of our knowledge, such signal isolation has not been reported so far using the TWINS-based implementation, apart from our recent study, where we employed PC.[22] As we will show here, PC is actually not required and all the desired signals can be isolated in partially collinear 2DES without any PC.

Indeed, important steps in this direction have already been reported for shaper-based 2DES.[40] Hamm and Zanni noted that, in principle, for shaper-based 2D-IR spectroscopy, all desired signals can be obtained "*from a single absorptive 2D IR spectrum without any phase cycling* ...."[14] Experimentally, Tan and co-workers employed a two-step PC scheme to separate R and NR signal contributions.[34,40] Such a scheme may, in principle, be replaced by pump pulse chopping,[40,50] as is usually done in TWINS-based 2DES to record differential transmission or reflectivity signals.[43,51]

Here, we build upon this earlier work to show how to disentangle all accessible quantum pathways and other signal contributions for 2DES in the partially collinear pump–probe geometry without PC. This procedure is demonstrated using data of a molecular J-aggregate,[22,52] which allows us to also apply the procedure to extract 0Q and 2Q signals of the excitonic material. This data evaluation strategy is straightforward and robust and can be used to reanalyze existing 2DES data.

II. RESULTS AND DISCUSSION

A. Partially collinear 2DES

1. Experimental setup

Ultrafast 2DES is performed utilizing pulses generated in a home-built noncollinear optical parametric amplifier (NOPA) and by using a TWINS[38] interferometer to generate the phase-stable pump pulse pair. We refer to Refs. 7 and 52 for further details. In short, broadband pulses covering a range from ~650 to 900 nm are generated using a NOPA[52,53] providing ~10 fs pulse duration[22] (FWHM of the intensity profile). The NOPA is pumped by a Yb:KGW laser (Carbide, Light Conversion) operating at 200 kHz repetition rate. In the partially collinear 2DES setup, a TWINS interferometer creates the inherently phase-stable excitation pulse pair with a delay τ. The pump pulse pair and the probe, delayed by the waiting time T, are focused onto the sample under a small angle, and the reflected probe is sent to a grating spectrograph (Acton SP-2150i, Princeton Instruments), as shown in Fig. 1(a). Differential spectra,

$$\frac{\Delta R}{R}(\tau, T, E_{det}) = \frac{S_{on}(\tau, T, E_{det}) - S_{off}(E_{det})}{S_{off}(E_{det})}, \tag{1}$$

are recorded as a function of inter-pulse delays τ between pump 1 and pump 2 and T between the second pump and the probe, as well as the detection energy E_{det}. The pump beam is modulated using a mechanical chopper wheel (MC2000B, Thorlabs) with 50 kHz, and probe spectra are recorded using a fast and sensitive line camera (AViiVA EM4, e2v) that records spectra at 100 kHz. This is how the nonlinear signal is isolated from recorded probe spectra with pump (S_{on}) and without pump (S_{off}). This pump pulse chopping fulfills the same function as the two-step PC with

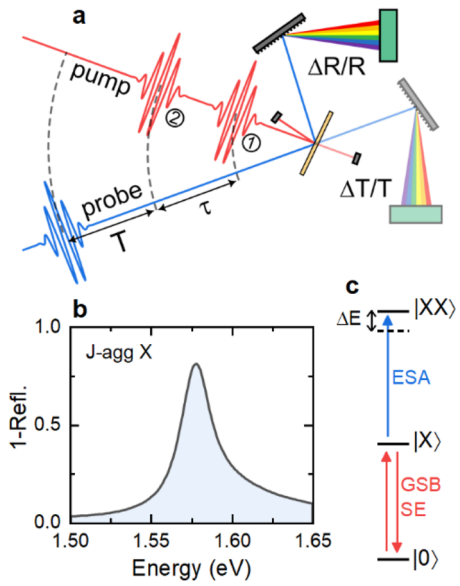

FIG. 1. (a) Schematic of 2DES in the pump–probe geometry. A collinear phase-stable pump pulse pair with variable delay τ (coherence time) excites the sample, followed by a probe pulse that is delayed by the waiting time T relative to the second pump pulse under a small angle relative to the pump beam. Depending on the investigated sample, either the transmitted or the reflected probe is dispersed in a spectrograph to measure the differential transmission $\Delta T/T$ or reflectivity $\Delta R/R$ as a function of the detection energy E_{det}. (b) Absorption, taken as 1–reflectivity, of a 10-nm squaraine-based molecular J-aggregate thin film on a gold substrate, referenced to the gold substrate. (c) Level scheme of the J-aggregate sample. The aggregate excitons behave as an effective three-level system with one- and two-exciton states $|X\rangle$ and $|XX\rangle$, respectively. A small blueshift of the $|XX\rangle$ state originates from Pauli blocking of the lowest energy exciton state in the aggregates. The sample is measured in reflectivity but, due to the gold substrate, is yielding absorption-type signals.

$\phi_{01} = [0, \pi]$ used, e.g., by Zhang *et al.*,[40] although with a comparatively reduced signal-to-noise ratio and additional transient absorption signal contributions.[34] Using the TWINS interferometer, the coherence time τ can be scanned for both positive and negative values; in our case, we choose a delay of ~230 fs in both directions. During such a τ-scan, performed for a fixed waiting time T, differential spectra are recorded on the fly, and at the same time, a linear autocorrelation $AC(\tau)$ of a small fraction of the excitation pulse pair is recorded using a photodiode. This autocorrelation measurement allows for the precise determination of $\tau = 0$ and for measuring the phase difference $\Delta\phi_{21}(E_{ex}) = \phi_2(E_{ex}) - \phi_1(E_{ex})$[22] of the pump pulse pair, which can be used for phase-correcting the 2DES data. Both the 2DES signal $A'_{2D}(E_{ex}, T, E_{det})$ and the excitation spectrum $I_{ex}(E_{ex})$, including the spectral phase difference between the excitation pulses, are obtained via a FT[15,43,54] along the τ-axis via

$$A'_{2D}(E_{ex}, T, E_{det}) = \int_{-\infty}^{\infty} \Theta(\tau) \frac{\Delta R}{R}(\tau, T, E_{det}) e^{i\frac{E_{ex}}{\hbar}\tau} d\tau \qquad (2)$$

and

$$I_{ex}(E_{ex}) = |I_{ex}(E_{ex})| e^{i\Delta\phi_{21}(E_{ex})} = \int_{-\infty}^{\infty} AC(\tau) e^{i\frac{E_{ex}}{\hbar}\tau} d\tau, \qquad (3)$$

respectively, with a Heaviside step function $\Theta(\tau)$ and Planck's reduced constant $\hbar$. In the numerical implementation, the first data point should be scaled by a factor of 1/2, which is usually already included in $\Theta(\tau)$, in order to avoid spurious background artifacts.[14,55] When taking the real part of the 2DES spectrum, $\Re\left(A'_{2D}(E_{ex}, T, E_{det})\right)$, we obtain the absorptive 2DES signal that contains both R and NR contributions in the form of energy–energy maps for each waiting time.[1,14] As the delay introduced in a TWINS interferometer is determined by the birefringence of the employed crystals, it is color-dependent. To calibrate the E_{ex} axis, the spectrum of the pump pulse pair is measured as a function of τ in the same manner as for a 2DES scan and then Fourier transformed, yielding the modulation frequency induced by the TWINS for each E_{ex} in the pump spectrum.[22,38]

2. Molecular J-aggregate sample

To demonstrate the isolation of the different signal contributions, we choose a molecular J-aggregate,[8,52,56,57] based on quadrupolar squaraine[58,59] molecules, as the investigated sample. The deposition of the squaraine molecule ProSQ-C16 dissolved in chloroform on gold-coated substrates via spin coating results in thin films with ~10-nm thickness that are subsequently annealed to enhance their optical properties.[52,58] The resulting aggregates show a sharp and strong superradiant exciton peak close to 1.58 eV [Fig. 1(b)] resulting from dipolar coupling between the molecular excitations, delocalizing the excitons across at least 24 monomers.[52,56] Their large dipole moment makes molecular aggregates an interesting excitonic material for strong coupling experiments.[8,10,60] Importantly, in a previous study, we could confirm that such J-aggregated thin films are effective three-level systems (3LS) arising from an exciton to two-exciton ($|X\rangle \rightarrow |XX\rangle$) transition[52,56,61,62] that is blueshifted by ~3 meV due to the Pauli blocking of the lowest energy two-exciton state [Fig. 1(c)].[22] Using PC with the TWINS interferometer, we measured isolated R, NR, 0Q, and 2Q signals and were able to achieve good agreement with simulations based on a perturbative description using response functions for such a 3LS.[22]

The aggregated squaraine is deposited on a highly reflective gold surface. For such a sample, the differential reflectivity $\Delta R/R$ mainly probes the pump-induced change in the absorption of the thin film, i.e., the imaginary part of the nonlinear sample susceptibility $\chi^{(3)}$. In this geometry, the reflected probe pulse effectively passes twice through the thin film before it is re-emitted from the sample.[7,52] This results in an absorptive line shape of the linear reflectivity [Fig. 1(b)], as confirmed by finite difference time domain simulations for such a sample geometry.[8] Usually, differential transmission signals $\Delta T/T$ are associated with the imaginary part of susceptibility,[14] while experiments in reflection probe its real part.[63] This, however, holds true only for homogeneous samples, while for stacked layers, a full transfer matrix calculation is needed.

3. The measured signal

To rationalize the measured signals, we employ a perturbative description of the third order nonlinear response based on response functions.[14,15] In the three-pulse experiment, assuming δ-pulses, we can describe the 2DES signal in the time-domain via a sum of relevant response functions,

$$A_{2D}(\tau, T, t) = \sum_j iR_j(\tau, T, t) + (iR_j(\tau, T, t))^*, \qquad (4)$$

that contain also the complex conjugate term, making $A_{2D}(\tau, T, t)$ real-valued. The prefactor of i reflects a 90° phase lag between the measured signal field and the sample response resulting from the absorption-type measurement geometry.[4,14,64] Due to the causality,[49] these response functions are only defined for positive times t, implying that the nonlinear field is only emitted after the interaction of the third pulse with the sample. The response function depends on the ordering of the pulses, and we first consider here the case for single-quantum 2DES with the pulse ordering pump 1, pump 2, and probe, and therefore, $\tau, T, t > 0$. In this case, the signal is emitted into the probe direction due to the phase matching condition $\vec{k}_{sig} = \pm\vec{k}_1 \mp \vec{k}_2 + \vec{k}_3$, where $\vec{k}_i$ is the wave vector that is associated with the ith field interaction. The system response can be divided into two different classes of response functions, the R and NR contributions, which are characterized by their phase evolution along τ and t,

$$R_R(\tau, T, t) \propto \Theta(t) i^3 e^{+i(\omega_X - \omega_0)\tau - \gamma\tau} e^{-\kappa T} e^{-i(\omega_X - \omega_0)t - \gamma t}, \qquad (5)$$

$$R_{NR}(\tau, T, t) \propto \Theta(t) i^3 e^{-i(\omega_X - \omega_0)\tau - \gamma\tau} e^{-\kappa T} e^{-i(\omega_X - \omega_0)t - \gamma t}, \qquad (6)$$

with $\hbar(\omega_X - \omega_0)$ being the energy difference between the ground state $|0\rangle$ and the excited state $|X\rangle$, γ being the 1-quantum dephasing rate, and κ being the population relaxation rate. These responses correspond to stimulated emission (SE) and ground state bleaching (GSB) pathways. Additional response functions for an excited state absorption (ESA) will evolve with the energy difference between the first and second excited states $\hbar(\omega_{XX} - \omega_X)$ during t instead. For simplicity, we restrict our description to phenomenological exponential dephasing. The discussed response functions can, however, also easily be extended to include line shapes

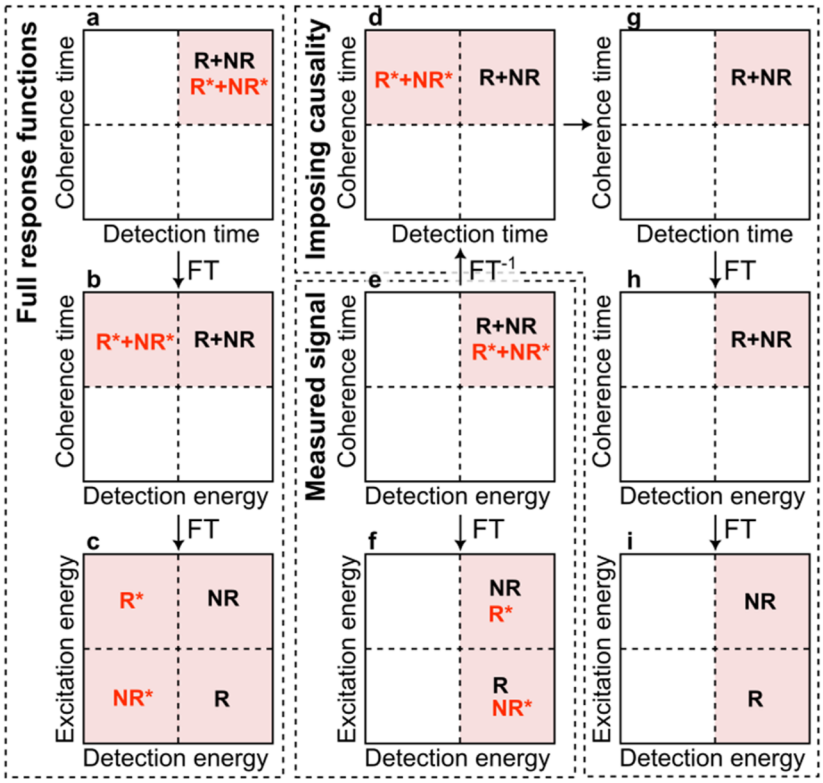

FIG. 2. Strategy to disentangle R and NR contributions in partially collinear 2DES. (a)–(c) Location of R, NR, R*, and NR* signal contributions in different quadrants when starting with the real-valued signal in the time domain (a) and after subsequent FT along t (b) and τ (c). Here, all contributions reside in separate spectral quadrants. (e) Real-valued 2DES signal as measured in a coherence time scan. (f) After FT along τ, R*+NR and R+NR* are located in the two spectral excitation energy quadrants. (d) and (g)–(i) Isolating R and NR via imposing causality. Inverse FT along t (d) separates the response functions and their complex conjugate in the time domain. After removing the signal for $t < 0$ (g) and subsequent FT along t (h) and τ (i), R and NR are now spectrally isolated.

that result from a more sophisticated description of system–bath interactions.[14,15]

Causality implies that the 2DES signal $A_{2D}(\tau, T, E_{det})$ that results from these response functions, after being Fourier transformed along the detection time t, will be complex-valued and Hermitian, meaning that the complex conjugate of the function is equal to the function at opposite values of E_{det}. The contributions from R_R and R_{NR} to these signals are then located at positive detection energies according to their phase evolution during t, while the complex conjugate responses R_R^* and R_{NR}^* will be located at negative detection energies [Figs. 2(a) and 2(b)]. In Fig. 2, these contributions are labeled R, R*, NR, and NR*, respectively. Subsequent FT along τ will yield a complex-valued $A_{2D}(E_{ex}, T, E_{det})$. This further separates R_R and R_{NR} into different quadrants along the excitation energy axis according to their phase evolution during τ in Eqs. (5) and (6). As a result, they reside at $(-E_{ex}, +E_{det})$ and $(+E_{ex}, +E_{det})$, respectively [Fig. 2(c)]. In contrast, the contribution of the conjugate signals R_R^* and R_{NR}^* will be located in opposite quadrants at $(+E_{ex}, -E_{det})$ and $(-E_{ex}, -E_{det})$, respectively.

In our experimental realization, however, the 2DES signal is not recorded in the time domain, but instead the spectrometer measures only the real part of the complex-valued $A_{2D}(\tau, T, E_{det})$ for positive detection energies, i.e.,

$$\begin{aligned} A'_{2D}(\tau, T, E_{det}) &= 2\Re(A_{2D}(\tau, T, E_{det})) \\ &= 2\Re(iR_R(\tau, T, E_{det}) + iR_{NR}(\tau, T, E_{det})) \\ &= iR_R(\tau, T, E_{det}) + iR_{NR}(\tau, T, E_{det}) \\ &\quad - iR_R^*(\tau, T, E_{det}) - iR_{NR}^*(\tau, T, E_{det}) \\ &= R + NR + R^* + NR^*. \end{aligned} \tag{7}$$

The factor of 2 arises from A'_{2D} being the interference term between the nonlinear electric field and the probe. We express the real part of the complex nonlinear signal by adding its complex conjugate and using Eq. (4) to express the signal in terms of the rephasing and non-rephasing contributions. Therefore, the measured coherence time scan does not only carry information about R and NR but also carry information about the complex conjugate R* and NR* terms, as visualized in Fig. 2(e). Now, FT along τ separates the contributions in such a way that R*+NR is located in the $(+E_{ex}, +E_{det})$ quadrant, while R+NR* is located at $(-E_{ex}, +E_{det})$, as shown in Fig. 2(f). When taking the real part, both quadrants contain the real part of R and NR, giving rise to the conventional absorptive 2DES signal.

B. Imposing causality

A commonly employed strategy to recover isolated R and NR contributions in partially collinear 2DES is PC.[22,34,40] Such PC would require changing the relative absolute phases between the excitation pulses and also between the emitted signal field and the local oscillator.[14,34] A phase-stable excitation pulse pair for 2DES can readily be obtained by using a shaper[34,40] or TWINS.[22] The phase between the signal and the local oscillator (the probe pulse), however, cannot be varied conveniently.[14,34] Ogilvie and co-workers

have shown that this problem can be circumvented by making use of the causality of the nonlinear response.[34] The missing imaginary component of the measured $A'_{2D}(\tau, T, E_{det})$ signal, which is canceled by the additional R* and NR* contributions, can be reconstructed via imposing causality after inversely Fourier transforming A'_{2D} along E_{det}. In the time domain, $A'_{2D}(\tau, T, t)$ now contains signal for both positive and negative detection times [Fig. 2(d)], separating R and NR from their complex conjugate. This implies that R and NR can be isolated by "imposing causality," i.e., by applying a Heaviside step function, which effectively removes the contributions for negative t from the signal [Fig. 2(g)]. Subsequent FT along t and τ [Figs. 2(h) and 2(i)] then results in the 2DES signal $A^{caus}_{2D}(E_{ex}, T, E_{det})$ with R and NR separated in the two quadrants at $(-E_{ex}, +E_{det})$ and $(+E_{ex}, +E_{det})$, respectively. Evidently, R and NR can be separated without the need for PC. This result has already been shown, albeit possibly somewhat indirectly, by Tan and co-workers for shaper-based 2DES.[40] In most previous studies, however, additional PC is used to further isolate R and NR,[22,34,50] resulting in the other spectral quadrant being void of any signal. Such an additional step is actually not required in case that R and NR are always located in one quadrant only, i.e., when R and NR are not spectrally overlapping, which is not necessarily the case for shaper-based 2DES when measuring in the rotating frame or in case of undersampling along τ.[40] For TWINS, operating in a partially rotating frame, this condition is usually fulfilled if undersampling is avoided. For the data presented in this work, no PC has been applied.

To further illustrate the principle of imposing causality, Fig. 3 shows the application of this method to a real-valued Lorentzian resonance $L(E_{det}) = \Im(E_L - E_{det} - i\hbar\gamma)^{-1}$ in analogy to the measured (real-valued) absorptive signal. After inverse FT to the detection time domain, the Heaviside step function is applied, and when going back to the spectral domain, the imaginary component is recovered. This procedure is equivalent to computing the inverse Hilbert transform (HT) of the Lorentzian resonance [Fig. 3(d), blue dashed line]. This result is obtained since the real and imaginary components of the causal response are linked via a Kramers–Kronig relationship.[14,34] Importantly, the imaginary component retrieved by this HT does not always reproduce the result obtained by an independent measurement since the spectral bandwidth of the provided real part may be limited.[34] The HT, therefore, only reproduces the imaginary part arising from resonances that are sufficiently well covered experimentally, yet does not account for contributions that could arise from additional resonances outside the recorded spectral range.

We now apply this strategy to recover R and NR spectra for the molecular J-aggregate in Fig. 4. If $A'_{2D}(\tau, T, E_{det})$, shown in Fig. 4(a), is directly Fourier transformed along τ, the conventional absorptive 2DES map is obtained [Figs. 4(b) and 4(c)], yielding $\Re\{R + NR\}$. It shows a diagonal feature with a dispersive line shape along the detection at the $|X\rangle$ resonance close to 1.58 eV, reflecting positive SE and GSB contributions superimposed with a negative ESA of the $|X\rangle \rightarrow |XX\rangle$ transition,[56,61] blueshifted by ~3 meV.[22,52] The imaginary part [see Figs. 4(d) and 4(e)] is usually omitted, because the complex-conjugation of only the R or NR contribution is causing a line shape twist. Figures 4(c)–4(e) show the real and imaginary parts of the signal in the negative half of the E_{ex} axis. Since the measured data are real-valued, their Fourier transform is Hermitian. Thus, the negative E_{ex} half of the data is the complex-conjugate mirror image

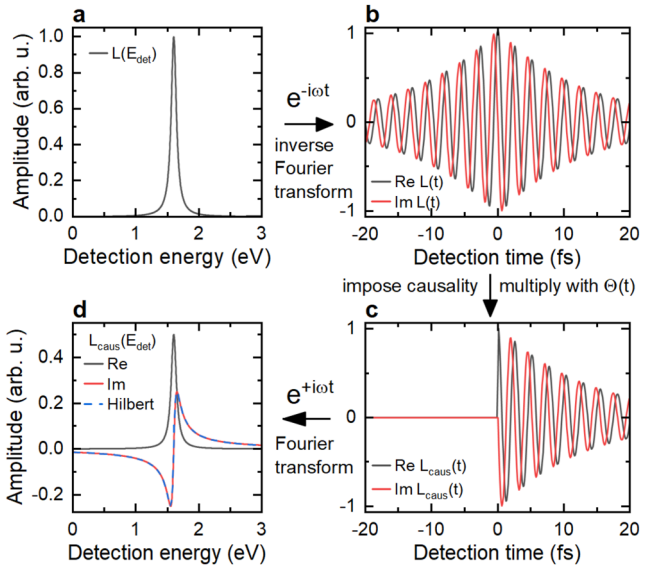

FIG. 3. Imposing causality for a Lorentzian $L(E_{det})$. (a) Imaginary part of the Lorentzian resonance at E_L = 1.58 eV, corresponding to a linear absorption measurement. (b) An inverse FT yields the complex-valued time-domain response. Based on causality, the signal for negative detection times can be removed. (c) Imposing causality via the Heaviside step function $\Theta(t)$ yields a causal signal. The first data point is multiplied by a factor of 1/2. (d) Fourier transforming back to the detection energy results in a complex response and recovers the imaginary part of the Lorentzian resonance (red line), while the real part of the response (black line) corresponds to the original signal multiplied by 1/2. This procedure is equivalent to adding the inverse Hilbert transform (blue dashed line) of the original, real-valued signal as its imaginary part (except for a factor of 1/2).

of the positive E_{ex} quadrant and thus does not yield additional information. This changes once the imaginary part of the measurement is recovered by imposing causality, as is displayed in Fig. 4(f). FT of this complex signal $A^{caus}_{2D}(\tau, T, E_{det})$ yields the desired spectrally isolated (complex-valued) R and NR signals [see Figs. 4(g)–4(j)]. Note that these two are no mirror images and thus provide independent information, namely the complex R and NR signal contributions, matching those previously reported for phase-cycled data and the perturbative simulations for the J-aggregate 3LS.[22] One can note that the assumptions that were made to obtain these signals are the same as for those signals obtained from phase-cycled data in partially collinear 2DES, which also require the same causality imposing.

C. Phase correction

When using the TWINS interferometer, the relative spectral phase $\Delta\phi_{21}(E_{ex})$ between the excitation pulses can deviate from zero, either unintentionally due to manufacturing tolerances of the optical components or their misalignment, or intentionally for PC.[22] The recorded absorptive 2DES data are sensitive to this phase, and both knowledge of $\Delta\phi_{21}(E_{ex})$ and phase-correction of the 2DES data are, therefore, highly desirable. As discussed above, a linear autocorrelation of the excitation pulse pair $AC(\tau)$ provides such access to the spectral phase[43,51] [Eq. (3)] and can be used to correct the 2DES data via

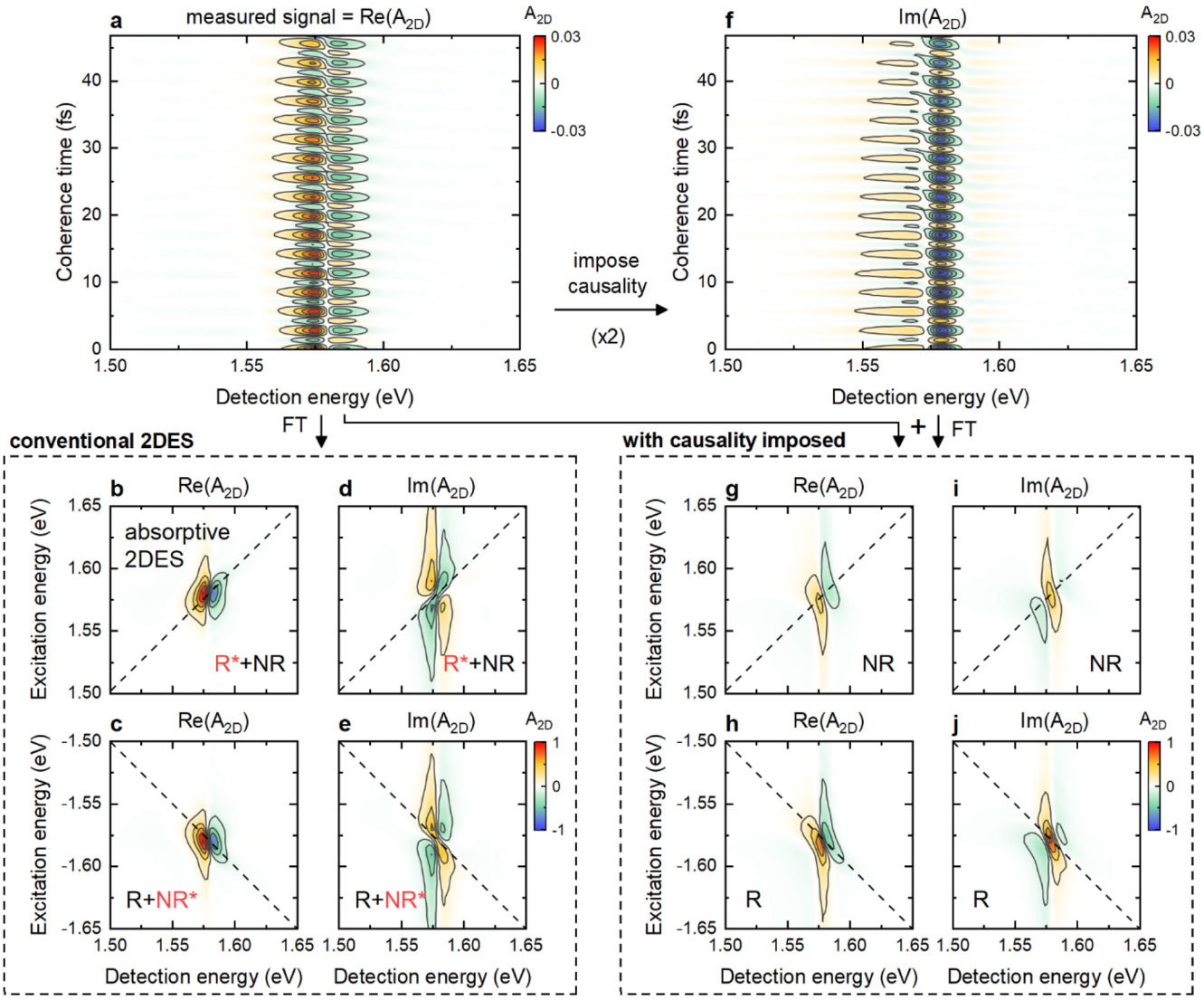

FIG. 4. Signals contained in spectrally recorded 2DES data in the partially collinear pump–probe geometry. (a) Experimental coherence time scan $A'_{2D}(\tau, T, E_{det})$ for the molecular J-aggregate shown in Fig. 1 for $T = 0$ fs. The group delay between the excitation pulses at 800 nm is taken as the coherence time τ. The data are recorded for τ up to ~260 fs. A Fourier transform yields the 2DES energy–energy maps $A'_{2D}(E_{ex}, T, E_{det})$. (b) and (c) Real part of the 2DES maps for positive and negative excitation energies. The map shown in b) is usually referred to as the absorptive 2DES map. (d) and (e) Corresponding imaginary contributions. Note that while the real parts are just mirrored along the $E_{ex} = 0$ line, the imaginary parts are also sign-flipped. (f) By imposing causality (Fig. 3), the imaginary contribution of the coherence time scan is recovered. (g)–(j) 2DES maps as in (b)–(e) but now after using the full complex-valued coherence time scan $A^{caus}_{2D}(\tau, T, E_{det})$. As a result, the maps show individual and isolated R and NR contributions, separated in different spectral quadrants. This is enabled by removing the complex conjugate contributions.

$$A^{corr}_{2D}(E_{ex}, T, E_{det}) = A'_{2D}(E_{ex}, T, E_{det}) e^{-i\Delta\phi_{21}(E_{ex})}. \quad (8)$$

As the FT spectrum of the measured 2DES map is Hermitian, the signal contained in $(-E_{ex}, +E_{det})$ is corrected by the conjugate phase compared to the signal in $(+E_{ex}, +E_{det})$. Such data correction also alleviates possible phase artifacts due to imprecise determination of $\tau = 0$. In case of the NR and R* signal pathways, the sample interacts with the field of the first pump pulse and with the conjugate field of the second pump pulse.[14] For the R and NR* signals, the sample interacts with the conjugate field of the first pump pulse and with the regular field of the second pump pulse. The phase imprinted on the signals is thus the difference of the individual pump pulse phases, $\Delta\phi_{R/NR}(E_{ex}) = \Delta\phi_{21}(E_{ex})$. Since in the case of the absorptive 2DES signal, R*+NR and R+NR* are located in the positive and negative excitation energy quadrants, respectively, the phase correction can be used on the conventional 2DES data. In the case of the causality imposed data $A^{caus}_{2D}(E_{ex}, T, E_{det})$, the same phase correction procedure can be used since the phase $\Delta\phi_{21}$ that corrects the NR

contribution is conjugate to that for the R signal. The fact that all effects of $\Delta\phi_{21}(E_{ex})$ can be undone in the data analysis further illustrates why there is no need to actually perform PC to isolate the 2DES signals.

D. Scattering contributions

The scattering of pump light into the direction of the probe beam is a known complication in 2DES spectroscopy. As it can overshadow diagonal peaks, its removal is desirable. There are two contributions to scattering signals, the intensity of the scattered excitation light and the interference between the scattered excitation pulse pair and the probe. Both contributions are modulated by $\left[1+\cos\left(E_{ex}\hbar^{-1}\tau\right)\right]$, resulting in a diagonal feature in the 2DES map (Fig. 5). The scattered excitation light is independent of T and usually much weaker than the second interference term. Due to its interferometric origin, this second term shows a spectral modulation that depends on T. In case that the coherence between the scattered pump light and the measured 2DES signal is suppressed, as can be achieved using PC or by modulating the pump–probe delay using a piezoelectric mirror,[51,65] this interference term is absent and only the T-independent term remains. Fourier transform of the scattering signal along τ yields three distinct features, of which all display the scattering spectrum as a line in the 2DES map: on the $E_{ex}=0$ line, on the $E_{ex}=E_{det}$ diagonal, and on the $E_{ex}=-E_{det}$ diagonal. The latter two can superimpose with the experimental 2DES signals as can be seen in a recorded pump pulse interferogram in Figs. 5(a) and 5(b), mimicking the effect of strong and broadband sample scattering.

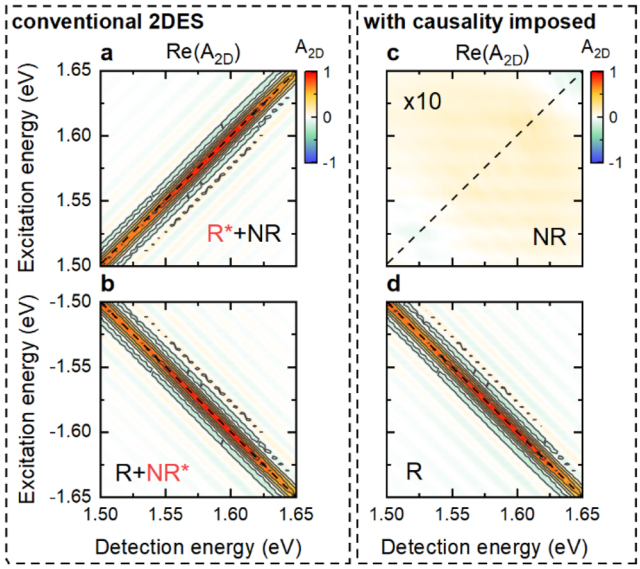

FIG. 5. Effect of imposing causality on scattering contributions. A 2DES calibration scan of the pump–pulse pair is evaluated the same way as the 2DES data in order to demonstrate the effect of scattering. (a) and (b) In conventional absorptive 2DES, scattering of the pump pulses results in a diagonal contribution to the 2DES data, for both positive and negative excitation energies. (c) and (d) By imposing causality, scattering signals are mostly located in one spectral quadrant, i.e., at negative excitation energies.

The scattering signal is of similar spectral shape as the nonlinear response of a strongly inhomogeneously broadened sample. Due to its real-valued cosine-type signal along τ, it contains both positive and negative frequency components. The antidiagonal linewidth is limited by the maximum coherence time τ_{max} used in experiment, while the extent along the diagonal is defined by the spectral bandwidth of the scattering spectrum. After imposing causality, the R contribution is, therefore, much stronger than the NR contribution, as shown in Figs. 5(c) and 5(d), where the NR signal is scaled by a factor of 10. As will be discussed below, the same also holds for 0Q and 2Q signals. In case that the homogeneous linewidth is much smaller than the inhomogeneous broadening, which is given for sufficiently large τ_{max} or broadband scattering spectra, the R contribution closely follows that of the absorptive 2DES scattering signal [Figs. 5(b)–5(d)]. The much weaker NR signal is not restricted to the diagonal, but much more spectrally broadened. Care should be taken to exclude such scattering artifacts from the 2DES data.

Isolated scattering signals for 2DES data correction may be obtained for negative waiting times $T \ll -\tau_{max}$ that are sufficiently negative such that no 2DES signal is contained in the coherence time scan. Alternatively, chopping of the probe can be used to record isolated scattering on a single-shot basis, as may be required for dynamic scattering events.[43,66] Care must be taken though that the interference terms between the pump pulses and the probe are adequately suppressed in order to obtain a truly T-independent scattering signal.

E. Absorptive signal and imaginary component

One advantage that is usually associated with a partially collinear 2DES geometry is the automatic phasing of R and NR contributions in order to obtain absorptive signals, i.e., $\Re\left(A'_{2D}(E_{ex},T,E_{det})\right)$.[1,3] Figure 4(b) shows such an absorptive map, which was obtained in the partially collinear pump–probe geometry from a real-valued coherence time scan $A'_{2D}(\tau,T,E_{det})$. We can now reconstruct such a signal by adding the R* and NR contributions obtained from $A^{caus}_{2D}(E_{ex},T,E_{det})$. For this, the rephasing component is flipped along the $E_{ex}=0$ line, complex conjugated, and added to the NR contribution. The resulting maps in Figs. 6(a) and 6(b) are identical to those for the conventionally evaluated data in Figs. 4(b)–4(d). In addition, the absolute value of $A'_{2D}(E_{ex},T,E_{det})$ is shown in Fig. 6(c). Due to the distorted imaginary component, the absolute value shows a spectral node and is strongly elongated along the excitation axis. When using R and NR instead to reconstruct the signal, as shown in Figs. 6(d)–6(f), the imaginary part is free from such a phase twist and the absolute valued map shows a single diagonal peak without nodes that is much less spread along E_{ex}. Instead of such a flipping in the spectral domain, Ogilvie and co-workers use symmetrization of $A^{caus}_{2D}(\tau,T,E_{det})$ along τ in order to obtain R+NR in both spectral quadrants.[34] In case that such an absolute line shape is desired, it can alternatively be computed from the absorptive 2DES signal directly by obtaining the imaginary contribution via an inverse HT.

F. Double-quantum and zero-quantum 2DES

So far, the discussed signals were of the 1Q variety, arising from the pulse ordering pump 1, pump 2, and probe. In these

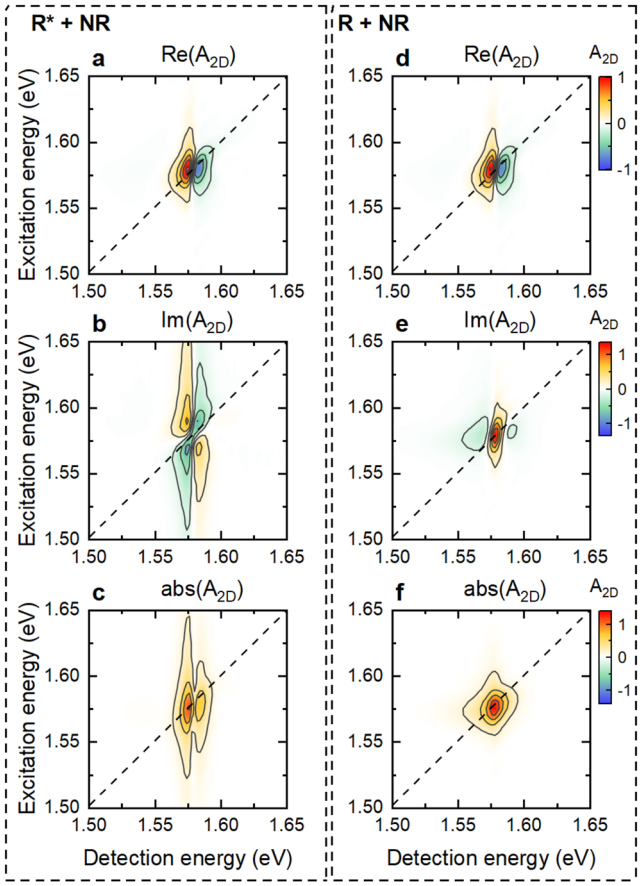

FIG. 6. Combining R and NR signals. (a)–(c) 2DES maps reconstructed from R*+NR, as in the experimentally recorded data shown in Figs. 4(b)–4(d). The imaginary component shows a distortion arising from the complex conjugation of the rephasing component. As a result, the absolute value of the 2DES signal is both sensitive to nodes in the signal and strongly spectrally broadened along the excitation energy axis. (d)–(f) When using R and NR instead, the same real values of the data are obtained but with a different imaginary contribution. Now, the phase twist is avoided, and as a result, the absolute 2DES signal is spectrally much more compact along the excitation energy and does not show a node in the amplitude.

pathways, the pump pulse pair excites the sample, i.e., it prepares the density matrix of the system in a population state.[14] However, 2DES also allows us to measure coherences between two states in the same ground or excited state manifold, separated by zero light quanta (0Q), and between the ground state and doubly excited states, separated by two light quanta (2Q).[2,21] In particular, the 2Q response requires interferometric phase stability between the second and third field interactions and fulfills phase matching of the form $\vec{k}_{sig} = \vec{k}_1 + \vec{k}_2 - \vec{k}_3$. In the pump–probe 2DES geometry, Cai *et al.* have shown that 0Q and 2Q signals can be recorded by changing the pulse ordering such that the first pump pulse interacts after the second pump and probe, which both interact with the sample at the same time.[41] This approach based on an adapted pulse ordering has also been introduced previously by the Zanni group for shaper-based 2D-IR spectroscopy.[67] This is schematically shown in Fig. 7(a).

In this case, the signal is emitted into the probe direction and the excitation pulse pair provides the relevant phase-stability between the second and third field interactions. In addition, there is phase stability between the probe field and the emitted nonlinear signal, even though they are not coinciding in time. While Zhang *et al.*[40] use a shaper-based approach and PC, 0Q and 2Q signals can be obtained in a similar fashion using the TWINS.[22] When keeping the labels introduced for the 1Q pulse ordering, this corresponds to $\tau < 0$ and $T = 0$, and thus, the desired data are contained in the coherence time scan for negative τ and zero waiting time [Fig. 7(b)], $\tilde{A}'_{2D}(\tau < 0, T = 0, E_{det})$. The 0Q and 2Q response functions are of the type[2,22]

$$R_{0Q}(\tau, T = 0, t) \propto \Theta(t) i^3 e^{-\kappa|\tau|} e^{-i(\omega_X - \omega_0)t - \gamma t}, \tag{9}$$

$$R_{2Q}(\tau, T = 0, t) \propto \Theta(t) i^3 e^{-i(\omega_{XX} - \omega_0)|\tau| - \gamma_{2Q}|\tau|} e^{-i(\omega_X - \omega_0)t - \gamma t}. \tag{10}$$

Additional responses that probe an ESA evolving with $(\omega_{XX} - \omega_X)$ during t, for both 0Q and 2Q, are not shown here. Since the nonlinear signal emission does not coincide with the probe field but happens after the third field interaction with pump 1, delayed by $|\tau| + T$ to the probe, the recorded 2DES signal accumulates a phase of $\exp[(iE_{det}(|\tau| + T))/\hbar]$, which acts as an effective rotation frame that depends on the detection energy.[22,41] 2Q signals are expected to reside close to $E_{2Q} \approx 2E_{det}$, while 0Q signals should be at zero energy, $E_{0Q} \approx 0$. The rotating frame shifts the 0Q and 2Q signals down along E_{ex} by the detection energy, and thus, 0Q signals reside in the $(-E_{ex}, +E_{det})$ quadrant, while 2Q signals are spectrally separated and located at $(+E_{ex}, +E_{det})$. However, due to the same reasons as for the R and NR contributions in 1Q 2DES, conjugate signals are superimposed in $\tilde{A}'_{2D}(E_{ex}, T = 0, E_{det})$, mixing the 0Q and 2Q contributions. They can, however, be separated in a similar fashion by imposing causality without any need for PC. The causality-imposed coherence time scan for the molecular J-aggregate, $\tilde{A}^{caus}_{2D}(\tau < 0, T = 0, E_{det})$, is shown in Figs. 7(b) and 7(c), and the 2DES maps resulting from FT along $|\tau|$ are presented in Figs. 7(d)–7(g).

Due to their shift along E_{ex}, the obtained 2DES maps do not yet provide accurate 0Q and 2Q signals.[22,41] To correct the E_{ex} axis, data have to be shifted up in excitation energy by E_{det},[22,41] as shown in Figs. 7(h)–7(k), yielding the correct 2Q and 0Q excitation energies,

$$E_{0Q/2Q}(E_{det}) = E_{ex} + E_{det}. \tag{11}$$

The waiting time T between the first and second pulses is set to zero to avoid system evolution and to prevent the effective rotating frame from influencing the signal. Experimentally, however, it may be challenging to set T to precisely zero. In case that there is a finite T due to experimental uncertainties, an additional phase is imprinted onto the data and may thus affect the 2DES maps. The frequency of this additional T-dependent phase evolution depends on the energy difference between the 1Q coherences that are induced by the first and third field interactions. Hence, this effect should be negligible if the uncertainty in T is sufficiently shorter than the period resulting from this energy difference.

Figures 7(h)–7(k) show the excitation energy-corrected 0Q and 2Q maps for the molecular J-aggregate, matching those reported previously.[22] The 2Q signal is a direct consequence of the 3LS, and

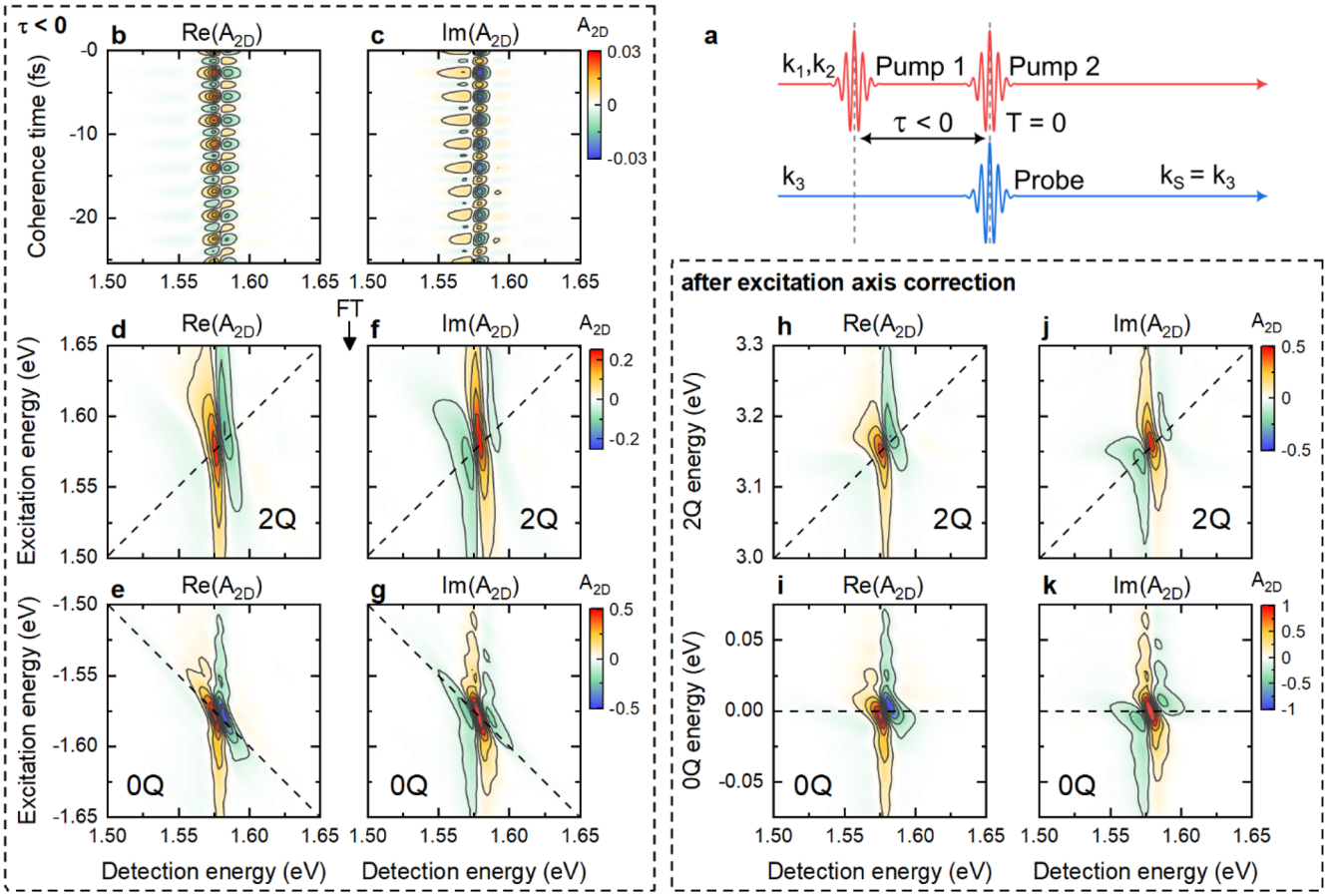

FIG. 7. Double- and zero-quantum 2DES in the partially collinear geometry. (a) Pulse sequence used in the experiment. In order for the third-order response to be emitted into the probe direction, the pulse ordering is changed such that for $T = 0$ fs, negative coherence times, $\tau < 0$, are scanned. (b) and (c) Real part (measured) and imaginary contribution (obtained via imposing causality) of the coherence time scan for $\tau < 0$, allowing us to gain access to 2Q and 0Q signals. (d)–(g) Real and imaginary contributions to the 2DES maps obtained after FT of $A_{2D}^{caus}(\tau < 0, T, E_{det})$. 2Q and 0Q signals are located in different spectral quadrants. (h)–(k) Since the third-order response is time-delayed to the heterodyning probe by τ, the signals are effectively measured in a rotating frame and require a correction of the excitation energy axis in order to obtain the correct 2Q and 0Q energies. Note that spectral oscillations along the excitation/0Q energy of the 0Q signals arise from the truncation of the signal due to a finite negative coherence time range of ~−230 fs.

its dispersive nature arises from the two-exciton blueshift.[22,23] The 0Q signal has similar GSB/SE and ESA contributions as the R 1Q contributions[2,22,41] and probes the J-aggregate lifetime and possible coherences in the excited or in the ground state.[22,27,68] Ripples along E_{0Q}, seen in Figs. 7(i)–7(k), are a result of truncation of the coherence time scan with $\tau_{max} \approx \pm 230$ fs. In a previous study,[22] we have deduced an effective exciton decay with $\kappa^{-1} \approx 140$ fs and a 2Q dephasing time $\gamma_{2Q}^{-1} \approx 30$ fs from the phase-cycled 0Q and 2Q data, respectively. The chosen length of the coherence time scan is, therefore, sufficient to probe the short-lived 2Q signal, but too short to clearly resolve an expected bi-exponential exciton decay on an ~100 fs and few-picosecond time scale.[8] A larger negative τ can be achieved for TWINS when varying its design; in particular, modifying the thickness of the Y-cut parallel faces birefringent block. While effects due to inhomogeneous broadening are weak in the investigated J-aggregate, 2Q spectra are also sensitive to energetic disorder via their peak shape.[69] In addition, 2Q-2DES is sensitive to correlations between fluctuations of the involved 2Q and 1Q transitions, which can be affected, for example, by many-body interactions. The excitonic substructure, expected from a Frenkel exciton model,[56] may also be obfuscated by such inhomogeneous broadening and rapid 2Q dephasing. 0Q peaks located at $E_{0Q} \neq 0$, a manifestation of coherent quantum beats that can arise from coherent couplings,[2,28] do not exist in the pristine J-aggregate investigated here, but may be of interest for strongly coupled hybrid systems[8,10] or quantum materials.[7] Since the coherence in conventional 2DES is usually scanned also for some finite negative range, already existing 2DES data may possibly be used to isolate 2Q signals. In our analysis, we found it helpful to identify spurious 0Q and 2Q signals arising from the substrate or solvent via reference measurements. In addition, it should be ensured that the waiting time is close to zero in order to avoid phase artifacts

and possible effects caused by a change in pulse ordering during the τ-scan.

III. CONCLUSION AND OUTLOOK

It is the aim of this paper to describe and discuss how to make use of the causality of nonlinear response functions for analyzing two-dimensional electronic spectra recorded in a partially collinear pump–probe geometry. For this, we build upon earlier work by Myers *et al.*[34] and Zhang *et al.*[40] and enforce causality on the 2DES data recorded in a partially collinear setup based on a TWINS interferometer. We perform this analysis on data recorded for a J-aggregated molecular thin film acting as an effective three-level system.[22] We show that by exploiting the causality constraints of the 2DES data, we can isolate rephasing, non-rephasing, zero-quantum, and double-quantum contributions with high fidelity from a single 2DES measurement. In addition, unwanted scattering contributions can be partially suppressed. This analysis avoids the need of commonly applied phase cycling schemes for obtaining this information, thus substantially simplifying the acquisition of the 2DES data. Even though the approach discussed here may not be compatible with some advanced acquisition schemes that are available for shaper-based 2DES, such as measuring in the rotating frame or undersampling, it provides access to the full scope of 2DES for the technologically simple pump–probe geometry without the need to apply PC. In particular, this data evaluation strategy can be used to reevaluate existing data and may allow for new perspectives and insights offered by the full realm of third-order nonlinear responses and beyond. In addition, we believe that it may also be helpful for the implementation of fully collinear 2DES geometries and ultrafast 2DES microscopy.

ACKNOWLEDGMENTS

We acknowledge the financial support from Deutsche Forschungsgemeinschaft (SFB 1372 magnetoreception and navigation in vertebrates, Project Nos. 395940726, INST 184/163-1, INST 184/164-1, Li 580/16-1, and DE 3578/3-1). We also acknowledge the financial support from the Niedersächsische Ministerium für Wissenschaft und Kultur (DyNano and Wissenschaftsraum ElLiKo) and the Volkswagen Foundation (SMART). G.C. acknowledges the financial support by the European Union's NextGenerationEU program with the i-PHOQS Infrastructure (Grant Nos. IR0000016, ID D2B8D520, and CUP B53C22001750006) "Integrated infrastructure initiative in Photonic and Quantum Sciences." We thank Jennifer Ogilvie and Howe-Siang Tan for helpful feedback on the manuscript.

AUTHOR DECLARATIONS

Conflict of Interest

The authors have no conflicts to disclose.

Author Contributions

D.T. and D.C.L. contributed equally to this work. **Daniel Timmer**: Conceptualization (equal); Formal analysis (equal); Investigation (equal); Methodology (equal); Software (equal); Supervision (equal); Visualization (equal); Writing – original draft (equal); Writing – review & editing (equal); **Daniel C. Lünemann**: Conceptualization (equal); Formal analysis (equal); Investigation (equal); Methodology (equal); Software (equal); Writing – original draft (equal); Writing – review & editing (equal). **Antonietta De Sio**: Funding acquisition (supporting); Resources (supporting); Supervision (equal); Validation (equal); Writing – review & editing (equal). **Giulio Cerullo**: Funding acquisition (supporting); Supervision (supporting); Validation (equal); Writing – review & editing (equal). **Christoph Lienau**: Funding acquisition (equal); Resources (equal); Supervision (equal); Validation (equal); Writing – review & editing (equal).

DATA AVAILABILITY

Data underlying the results presented in this paper are not publicly available at this time but may be obtained from the authors upon reasonable request.

REFERENCES

[1] E. Fresch, F. V. A. Camargo, Q. Shen, C. C. Bellora, T. Pullerits, G. S. Engel, G. Cerullo, and E. Collini, "Two-dimensional electronic spectroscopy," Nat. Rev. Methods Primers **3**(1), 84 (2023).

[2] H. Li, B. Lomsadze, G. Moody, C. Smallwood, and S. Cundiff, *Optical Multidimensional Coherent Spectroscopy* (Oxford University Press, 2023).

[3] F. D. Fuller and J. P. Ogilvie, "Experimental implementations of two-dimensional Fourier transform electronic spectroscopy," Annu. Rev. Phys. Chem. **66**, 667–690 (2015).

[4] J. D. Hybl, A. W. Albrecht, S. M. Gallagher Faeder, and D. M. Jonas, "Two-dimensional electronic spectroscopy," Chem. Phys. Lett. **297**(3–4), 307–313 (1998).

[5] J. Jeener, B. H. Meier, P. Bachmann, and R. R. Ernst, "Investigation of exchange processes by two-dimensional NMR spectroscopy," J. Chem. Phys. **71**(11), 4546–4553 (1979).

[6] C. L. Smallwood and S. T. Cundiff, "Multidimensional coherent spectroscopy of semiconductors," Laser Photonics Rev. **12**(12), 1800171 (2018).

[7] D. Timmer, M. Gittinger, T. Quenzel, A. R. Cadore, B. L. T. Rosa, W. Li, G. Soavi, D. C. Lünemann, S. Stephan, M. Silies, T. Schulz, A. Steinhoff, F. Jahnke, G. Cerullo, A. C. Ferrari, A. De Sio, and C. Lienau, "Ultrafast coherent exciton couplings and many-body interactions in monolayer WS_2," Nano Lett. **24**(26), 8117–8125 (2024).

[8] D. Timmer, M. Gittinger, T. Quenzel, S. Stephan, Y. Zhang, M. F. Schumacher, A. Lützen, M. Silies, S. Tretiak, J. H. Zhong, A. De Sio, and C. Lienau, "Plasmon mediated coherent population oscillations in molecular aggregates," Nat. Commun. **14**(1), 8035 (2023).

[9] M. Son, Z. T. Armstrong, R. T. Allen, A. Dhavamani, M. S. Arnold, and M. T. Zanni, "Energy cascades in donor–acceptor exciton–polaritons observed by ultrafast two-dimensional white-light spectroscopy," Nat. Commun. **13**(1), 7305 (2022).

[10] M. Russo, K. Georgiou, A. Genco, S. De Liberato, G. Cerullo, D. G. Lidzey, A. Othonos, M. Maiuri, and T. Virgili, "Direct evidence of ultrafast energy delocalization between optically hybridized J-aggregates in a strongly coupled microcavity," Adv. Opt. Mater. **12**(25), 2400821 (2024).

[11] N. Peruffo, F. Mancin, and E. Collini, "Coherent dynamics in solutions of colloidal plexcitonic nanohybrids at room temperature," Adv. Opt. Mater. **11**, 2203010 (2023).

[12] M. K. Yetzbacher, N. Belabas, K. A. Kitney, and D. M. Jonas, "Propagation, beam geometry, and detection distortions of peak shapes in two-dimensional Fourier transform spectra," J. Chem. Phys. **126**(4), 044511 (2007).

[13]X. Ma, J. Dostál, and T. Brixner, "Broadband 7-fs diffractive-optic-based 2D electronic spectroscopy using hollow-core fiber compression," Opt. Express **24**(18), 20781–20791 (2016).
[14]P. Hamm and M. Zanni, *Concepts and Methods of 2D Infrared Spectroscopy* (Cambridge University Press, 2011).
[15]S. Mukamel, *Principles of Nonlinear Optical Spectroscopy* (Oxford University Press, 1995).
[16]Y.-C. Cheng and G. R. Fleming, "Coherence quantum beats in two-dimensional electronic spectroscopy," J. Phys. Chem. A **112**(18), 4254–4260 (2008).
[17]X. Li, T. Zhang, C. N. Borca, and S. T. Cundiff, "Many-body interactions in semiconductors probed by optical two-dimensional Fourier transform spectroscopy," Phys. Rev. Lett. **96**(5), 057406 (2006).
[18]H. Li, S. A. Shah, A. R. S. Kandada, C. Silva, A. Piryatinski, and E. R. Bittner, "The optical signatures of stochastic processes in many-body exciton scattering," Annu. Rev. Phys. Chem. **74**, 467–492 (2023).
[19]Y. Song, C. Hellmann, N. Stingelin, and G. D. Scholes, "The separation of vibrational coherence from ground- and excited-electronic states in P3HT film," J. Chem. Phys. **142**(21), 212410 (2015).
[20]L. Bolzonello, A. Volpato, E. Meneghin, and E. Collini, "Versatile setup for high-quality rephasing, non-rephasing, and double quantum 2D electronic spectroscopy," J. Opt. Soc. Am. B **34**(6), 1223–1233 (2017).
[21]J. Kim, S. Mukamel, and G. D. Scholes, "Two-dimensional electronic double-quantum coherence spectroscopy," Acc. Chem. Res. **42**(9), 1375–1384 (2009).
[22]D. Timmer, D. C. Lünemann, M. Gittinger, A. De Sio, C. Manzoni, G. Cerullo, and C. Lienau, "Phase-cycling and double-quantum two-dimensional electronic spectroscopy using a common-path birefringent interferometer," Optica **11**, 1646 (2024).
[23]L. Bolzonello, F. Fassioli, and E. Collini, "Correlated fluctuations and intraband dynamics of J-aggregates revealed by combination of 2DES schemes," J. Phys. Chem. Lett. **7**(24), 4996–5001 (2016).
[24]T. M. Autry, G. Nardin, C. L. Smallwood, K. Silverman, D. Bajoni, A. Lemaître, S. Bouchoule, J. Bloch, and S. Cundiff, "Excitation ladder of cavity polaritons," Phys. Rev. Lett. **125**(6), 067403 (2020).
[25]M. A. Conway, J. B. Muir, S. K. Earl, M. Wurdack, R. Mishra, J. O. Tollerud, and J. A. Davis, "Direct measurement of biexcitons in monolayer WS_2," 2D Mater. **9**(2), 021001 (2022).
[26]D. Karaiskaj, A. D. Bristow, L. Yang, X. Dai, R. P. Mirin, S. Mukamel, and S. T. Cundiff, "Two-quantum many-body coherences in two-dimensional Fourier-transform spectra of exciton resonances in semiconductor quantum wells," Phys. Rev. Lett. **104**(11), 117401 (2010).
[27]K. Hao, G. Moody, F. Wu, C. K. Dass, L. Xu, C. H. Chen, L. Sun, M. Y. Li, L. J. Li, A. H. MacDonald, and X. Li, "Direct measurement of exciton valley coherence in monolayer WSe_2," Nat. Phys. **12**(7), 677–682 (2016).
[28]T. L. Purz, E. W. Martin, P. Rivera, W. G. Holtzmann, X. Xu, and S. T. Cundiff, "Coherent exciton–exciton interactions and exciton dynamics in a $MoSe_2/WSe_2$ heterostructure," Phys. Rev. B **104**(24), L241302 (2021).
[29]P. Malý, J. Lüttig, P. A. Rose, A. Turkin, C. Lambert, J. J. Krich, and T. Brixner, "Separating single-from multi-particle dynamics in nonlinear spectroscopy," Nature **616**(7956), 280–287 (2023).
[30]J. Lüttig, S. Mueller, P. Malý, J. J. Krich, and T. Brixner, "Higher-order multidimensional and pump–probe spectroscopies," J. Phys. Chem. Lett. **14**(33), 7556–7573 (2023).
[31]P. Brosseau, S. Palato, H. Seiler, H. Baker, and P. Kambhampati, "Fifth-order two-quantum absorptive two-dimensional electronic spectroscopy of CdSe quantum dots," J. Chem. Phys. **153**(23), 234703 (2020).
[32]S. Pres, B. Huber, M. Hensen, D. Fersch, E. Schatz, D. Friedrich, V. Lisinetskii, R. Pompe, B. Hecht, W. Pfeiffer, and T. Brixner, "Detection of a plasmon-polariton quantum wave packet," Nat. Phys. **19**(5), 656–662 (2023).
[33]S. Mueller, J. Lüttig, L. Brenneis, D. Oron, and T. Brixner, "Observing multiexciton correlations in colloidal semiconductor quantum dots via multiple-quantum two-dimensional fluorescence spectroscopy," ACS Nano **15**(3), 4647–4657 (2021).
[34]J. A. Myers, K. L. Lewis, P. F. Tekavec, and J. P. Ogilvie, "Two-color two-dimensional Fourier transform electronic spectroscopy with a pulse-shaper," Opt. Express **16**(22), 17420–17428 (2008).
[35]N. M. Kearns, R. D. Mehlenbacher, A. C. Jones, and M. T. Zanni, "Broadband 2D electronic spectrometer using white light and pulse shaping: Noise and signal evaluation at 1 and 100 kHz," Opt. Express **25**(7), 7869–7883 (2017).
[36]G. Bressan, I. A. Heisler, G. M. Greetham, A. Edmeades, and S. R. Meech, "Half-broadband two-dimensional electronic spectroscopy with active noise reduction," Opt. Express **31**(25), 42687–42700 (2023).
[37]J. Réhault, M. Maiuri, C. Manzoni, D. Brida, J. Helbing, and G. Cerullo, "2D IR spectroscopy with phase-locked pulse pairs from a birefringent delay line," Opt. Express **22**(8), 9063–9072 (2014).
[38]D. Brida, C. Manzoni, and G. Cerullo, "Phase-locked pulses for two-dimensional spectroscopy by a birefringent delay line," Opt. Lett. **37**(15), 3027–3029 (2012).
[39]H. Seiler, S. Palato, and P. Kambhampati, "Coherent multi-dimensional spectroscopy at optical frequencies in a single beam with optical readout," J. Chem. Phys. **147**(9), 094203 (2017).
[40]Z. Zhang, K. L. Wells, E. W. J. Hyland, and H. S. Tan, "Phase-cycling schemes for pump–probe beam geometry two-dimensional electronic spectroscopy," Chem. Phys. Lett. **550**, 156–161 (2012).
[41]M. R. Cai, X. Zhang, Z. Q. Cheng, T. F. Yan, and H. Dong, "Extracting double-quantum coherence in two-dimensional electronic spectroscopy under pump–probe geometry," Rev. Sci. Instrum. **95**(3), 033006 (2024).
[42]R. Borrego-Varillas, A. Oriana, L. Ganzer, A. Trifonov, I. Buchvarov, C. Manzoni, and G. Cerullo, "Two-dimensional electronic spectroscopy in the ultraviolet by a birefringent delay line," Opt. Express **24**(25), 28491–28499 (2016).
[43]D. Timmer, D. C. Lünemann, S. Riese, A. D. Sio, and C. Lienau, "Full visible range two-dimensional electronic spectroscopy with high time resolution," Opt. Express **32**(1), 835–847 (2024).
[44]S. E. Sanders, M. Zhang, A. Javed, and J. P. Ogilvie, "Expanding the bandwidth of fluorescence-detected two-dimensional electronic spectroscopy using a broadband continuum probe pulse pair," Opt. Express **32**(6), 8887–8902 (2024).
[45]Z. M. Faitz, D. Im, C. J. Blackwell, M. S. Arnold, and M. T. Zanni, "A spectrometer design that eliminates incoherent mixing signals in 2D action spectroscopies," J. Chem. Phys. **161**(13), 134202 (2024).
[46]S. Jana, S. Durst, and M. Lippitz, "Fluorescence-detected two-dimensional electronic spectroscopy of a single molecule," Nano Lett. **24**(40), 12576–12581 (2024).
[47]M. Aeschlimann, T. Brixner, A. Fischer, C. Kramer, P. Melchior, W. Pfeiffer, C. Schneider, C. Strüber, P. Tuchscherer, and D. V. Voronine, "Coherent two-dimensional nanoscopy," Science **333**(6050), 1723–1726 (2011).
[48]T. L. Purz, E. W. Martin, W. G. Holtzmann, P. Rivera, A. Alfrey, K. M. Bates, H. Deng, X. Xu, and S. T. Cundiff, "Imaging dynamic exciton interactions and coupling in transition metal dichalcogenides," J. Chem. Phys. **156**(21), 214704 (2022).
[49]R. W. Boyd, *Nonlinear Optics*, 3rd ed. (Academic Press, Inc., 2008).
[50]S. H. Shim and M. T. Zanni, "How to turn your pump–probe instrument into a multidimensional spectrometer: 2D IR and vis spectroscopiesvia pulse shaping," Phys. Chem. Chem. Phys. **11**(5), 748–761 (2009).
[51]J. Réhault, M. Maiuri, A. Oriana, and G. Cerullo, "Two-dimensional electronic spectroscopy with birefringent wedges," Rev. Sci. Instrum. **85**(12), 123107 (2014).
[52]T. Quenzel, D. Timmer, M. Gittinger, J. Zablocki, F. Zheng, M. Schiek, A. Lützen, T. Frauenheim, S. Tretiak, M. Silies, J. H. Zhong, A. De Sio, and C. Lienau, "Plasmon-enhanced exciton delocalization in squaraine-type molecular aggregates," ACS Nano **16**(3), 4693–4704 (2022).
[53]A. Grupp, A. Budweg, M. P. Fischer, J. Allerbeck, G. Soavi, A. Leitenstorfer, and D. Brida, "Broadly tunable ultrafast pump-probe system operating at multi-kHz repetition rate," J. Opt. **20**(1), 014005 (2018).
[54]W. H. Press, *Numerical Recipes 3rd Edition: The Art of Scientific Computing* (Cambridge University Press, 2007).
[55]G. Otting, H. Widmer, G. Wagner, and K. Wüthrich, "Origin of τ_1 and τ_2 ridges in 2D NMR spectra and procedures for suppression," J. Magn. Reson. (1969–1992) **66**(1), 187–193 (1986).
[56]J. Knoester, "Optical properties of molecular aggregates," in *Organic Nanostructures: Science and Applications* (IOS Press, 2002), pp. 149–186.
[57]D. Giavazzi, M. F. Schumacher, L. Grisanti, M. Anzola, F. Di Maiolo, J. Zablocki, A. Lützen, M. Schiek, and A. Painelli, "A marvel of chiral squaraine aggregates:

Chiroptical spectra beyond the exciton model," J. Mater. Chem. C **11**, 8307–8321 (2023).
[58]M. Schulz, J. Zablocki, O. S. Abdullaeva, S. Brück, F. Balzer, A. Lützen, O. Arteaga, and M. Schiek, "Giant intrinsic circular dichroism of prolinol-derived squaraine thin films," Nat. Commun. **9**(1), 2413 (2018).
[59]D. Timmer, F. Zheng, M. Gittinger, T. Quenzel, D. C. Lünemann, K. Winte, Y. Zhang, M. E. Madjet, J. Zablocki, A. Lützen *et al.*, "Charge delocalization and vibronic couplings in quadrupolar squaraine dyes," J. Am. Chem. Soc. **144**(41), 19150–19162 (2022).
[60]P. Vasa, W. Wang, R. Pomraenke, M. Lammers, M. Maiuri, C. Manzoni, G. Cerullo, and C. Lienau, "Real-time observation of ultrafast Rabi oscillations between excitons and plasmons in metal nanostructures with J-aggregates," Nat. Photonics **7**(2), 128–132 (2013).
[61]H. Fidder, J. Knoester, and D. A. Wiersma, "Observation of the one-exciton to two-exciton transition in a J aggregate," J. Chem. Phys. **98**(8), 6564–6566 (1993).
[62]A. Nemeth, F. Milota, T. Mančal, T. Pullerits, J. Sperling, J. Hauer, H. F. Kauffmann, and N. Christensson, "Double-quantum two-dimensional electronic spectroscopy of a three-level system: Experiments and simulations," J. Chem. Phys. **133**(9), 094505 (2010).
[63]X. T. Nguyen, D. Timmer, Y. Rakita, D. Cahen, A. Steinhoff, F. Jahnke, C. Lienau, and A. De Sio, "Ultrafast charge carrier relaxation in inorganic halide perovskite single crystals probed by two-dimensional electronic spectroscopy," J. Phys. Chem. Lett. **10**(18), 5414–5421 (2019).
[64]M. Sargent, M. O. Scully, and W. E. Lamb, *Laser Physics* (Addison-Wesley Pub. Co., Advanced Book Program, 1974).
[65]R. Bloem, S. Garrett-Roe, H. Strzalka, P. Hamm, and P. Donaldson, "Enhancing signal detection and completely eliminating scattering using quasi-phase-cycling in 2D IR experiments," Opt. Express **18**(26), 27067–27078 (2010).
[66]M. Son, S. Mosquera-Vázquez, and G. S. Schlau-Cohen, "Ultrabroadband 2D electronic spectroscopy with high-speed, shot-to-shot detection," Opt. Express **25**(16), 18950–18962 (2017).
[67]K. M. Farrell and M. T. Zanni, "Phase stable, shot-to-shot measurement of third- and fifth-order two-quantum correlation spectra using a pulse shaper in the pump–probe geometry," J. Chem. Phys. **157**(1), 014203 (2022).
[68]G. Nardin, G. Moody, R. Singh, T. M. Autry, H. Li, F. Morier-Genoud, and S. T. Cundiff, "Coherent excitonic coupling in an asymmetric double InGaAs quantum well arises from many-body effects," Phys. Rev. Lett. **112**(4), 046402 (2014).
[69]B. Lomsadze and S. T. Cundiff, "Line-shape analysis of double-quantum multidimensional coherent spectra," Phys. Rev. A **102**(4), 043514 (2020).